

Triazene drug metabolites. Part 16.¹ Kinetics and mechanism of the hydrolysis of aminoacyltriazenes

2 PERKIN

Emília Carvalho,^{*a} Jim Iley,^{*b} Maria de Jesus Perry^a and Eduarda Rosa^{*a}

^a CECF, Faculdade de Farmácia, Avenida das Forças Armadas, 1600 Lisboa, Portugal

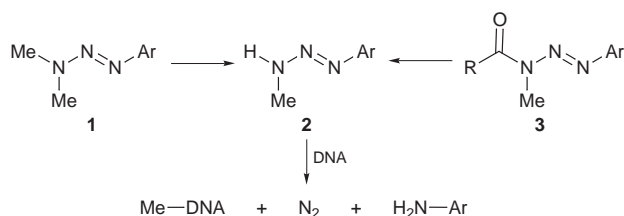
^b Chemistry Department, The Open University, Milton Keynes, UK MK7 6AA

Received (in Cambridge) 21st July 1998, Accepted 21st September 1998

Kinetic studies of the hydrolysis of 3-aminoacyl-1-aryl-3-methyltriazenes to the corresponding 1-aryl-3-methyltriazenes were carried out in pH 3–12 aqueous buffers at 25 °C. Pseudo-first-order rate constants were found to depend both on pH and buffer concentration. pH–Rate profiles for the compounds derived from α -amino acids, **3a–e**, exhibit sigmoidal curves consistent with an HO[−]-catalysed reaction proceeding *via* both protonated and unprotonated forms of the structure. For the β -amino acid derivative, **3f**, the difference in reactivity between these two substrate forms is much less pronounced. For the *N*-acetylated derivative, **3g**, only the unprotonated form is kinetically significant. Solvent deuterium isotope effects for the reaction of HO[−] with the protonated substrate are *ca.* 0.8 and for the unprotonated substrate *ca.* 1.0, suggesting nucleophilic catalysis by HO[−] for both forms. Both protonated and unprotonated forms of the substrate are subject to buffer catalysis. The Brønsted β value of 0.65 is consistent with general-base catalysis, as are the solvent deuterium isotope effect of *ca.* 1.3 for the imidazole-catalysed hydrolysis of the protonated substrate and the ratio of 1.1 for the piperidine- and 2,2,4,4-tetramethylpiperidine-catalysed hydrolyses of the unprotonated form.

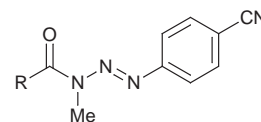
Introduction

1-Aryl-3,3-dimethyltriazenes **1** are antitumour compounds² that suffer oxidative *N*-demethylation by hepatic cytochrome P450 enzymes to give the cytotoxic 1-aryl-3-methyltriazenes **2**. These are known alkylating agents capable of alkylating DNA and RNA (Scheme 1).^{3,4} With the object of finding prodrugs



Scheme 1

of **2** that by-pass the need for oxidative metabolism, we have directed our attention to the 3-acyltriazenes **3**. Previously, we studied the deacylation of the R = alkyl and R = aryl analogues in basic ethanolic media⁵ and in sulfuric acid solutions⁶ and found that they decompose to give **2**. However, these compounds have low water solubility and too high a stability at pH = 7.4 for them to function as suitable prodrugs. In an attempt to circumvent these problems we have synthesised acyltriazenes derived from α -amino acids and studied their rates of hydrolysis in isotonic phosphate buffer and 80% human plasma.¹ These compounds are more reactive than their simple alkyl and aryl analogues, decomposing at pH 7.4 with half-lives ranging from 26 to 105 min. Increased hydrolytic reactivity due to the presence of an α -amino group has been observed before.^{7–13} In order to better understand the mechanism of hydrolysis of the aminoacyltriazenes, we have carried out a study of the kinetics of hydrolysis of compounds **3a–g** and herein report our results.



- 3a** R = CHMeNH₂ **3e** R = CH(CHMeEt)NH₂
3b R = CH(CH₂Ph)NH₂ **3f** R = CH₂CH₂NH₂
3c R = CH₂NH₂ **3g** R = CHMeNHAc
3d R = CHPrⁱNH₂

Results and discussion

In acidic solutions aminoacyltriazenes **3a–g** hydrolyse to give the corresponding anilines. In solutions of pH > 7 the intermediate formation of the monomethyltriazene **2** can be monitored. In these latter reactions, the hydrolysis of **3** can be monitored by following the reactions at the wavelength of the isobestic point for the decomposition of **2**; using this method good first-order plots were obtained. Pseudo-first-order rate constants, k_{obs} , for the hydrolysis of compounds **3a–g** were determined both in aqueous buffers using several buffer concentrations at each pH, and in NaOH solutions. The results obtained for compound **3a** (Tables 1 and 2) demonstrate clearly that k_{obs} is dependent upon both the pH of the solution and the buffer concentration. Similar results were obtained for the other substrates.

The hydroxide-catalysed reaction

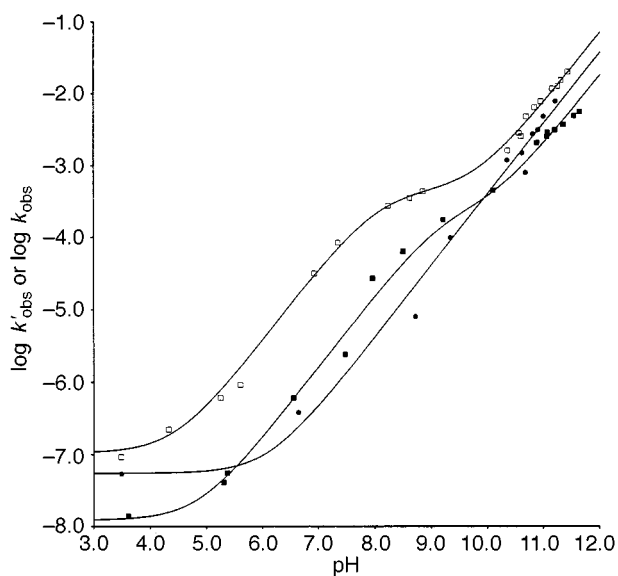
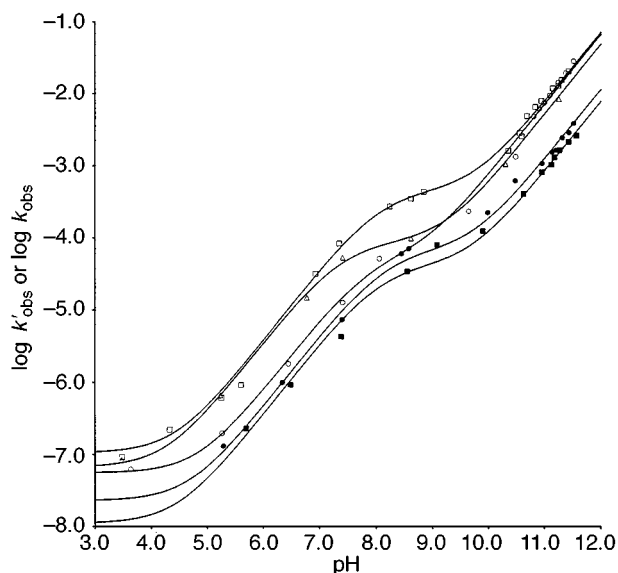
Using the intercepts, k'_{obs} , of plots of k_{obs} versus [buffer], together with the k_{obs} values determined in NaOH solutions, pH–rate profiles (Figs. 1 and 2) were constructed. Fig. 1 shows the effect of the type and position of the amino group. Compound **3a** exhibits a sigmoid-shaped curve, reflecting the protonated state of the α -amino group. Compound **3g**, in which the amino group is acetylated, exhibits a simpler profile involving a pH-independent rate below *ca.* pH 5, followed by

Table 1 Pseudo-first-order rate constants, k_{obs} , for the hydrolysis of **3a** in aqueous buffers at 25 °C

Buffer	[Buffer]/mol dm ⁻³	pH (pD)	$k_{\text{obs}}/10^{-5} \text{ s}^{-1}$	Buffer	[Buffer]/mol dm ⁻³	pH (pD)	$k_{\text{obs}}/10^{-5} \text{ s}^{-1}$
Formate	0.002	3.61	0.0092	Imidazole	0.02	(6.70)	0.0189
	0.007	3.48	0.0103		0.08	(6.61)	0.0199
	0.020	3.40	0.0112		0.16	(6.68)	0.241
	0.040	3.48	0.0134		0.20	(6.71)	0.300
	0.100	3.45	0.0197		0.25	(6.72)	0.332
Acetate	0.007	4.27	0.0233	Phosphate	0.0050	7.32	9.36
	0.020	4.33	0.0303		0.0125	7.36	10.80
	0.040	4.34	0.0375		0.0200	7.38	10.86
	0.080	4.36	0.0546		0.0250	7.29	11.30
	0.100	4.37	0.0635		0.0500	7.53	18.38
Pyridine	0.010	5.27	0.0633	Morpholine	0.015	8.16	29.3
	0.050	5.31	0.0803		0.100	8.24	31.7
	0.100	5.25	0.111		0.300	8.22	40.7
	0.200	5.27	0.158		0.400	8.30	44.3
	0.400	5.20	0.231		0.015	8.92	45.8
	0.024	6.19	0.206	0.10	8.95	52.0	
	0.056	6.11	0.221	0.20	8.92	61.0	
	0.110	6.12	0.252	0.30	8.94	66.5	
	0.170	6.03	0.286	Piperidine	0.01	10.71	1150
	Imidazole	0.01	6.48		0.657	0.02	10.81
0.02		6.53	0.675		0.03	10.88	1617
0.08		6.52	0.769		0.04	10.87	1807
0.16		6.50	0.893	0.01	10.89	2280	
0.20		6.51	1.03	0.02	10.99	2537	
				0.03	11.04	2833	
				0.04	11.11	3169	

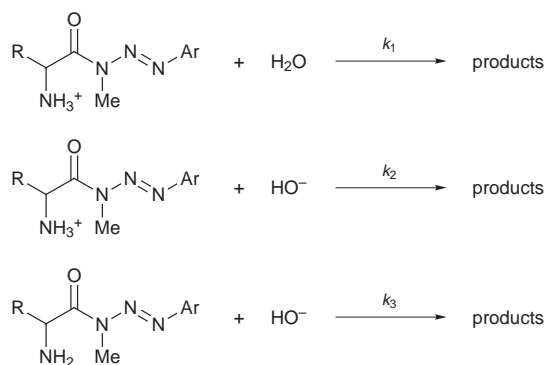
Table 2 Pseudo-first-order rate constants, k_{obs} , for the hydrolysis of **3a** and **3c** in sodium hydroxide solutions at 25 °C

	3a		3c		
	Conc./mol dm ⁻³	$k_{\text{obs}}/10^{-5} \text{ s}^{-1}$	Conc./mol dm ⁻³	$k_{\text{obs}}/10^{-5} \text{ s}^{-1}$	
NaOH	0.0005	516	NaOH	0.00065	510
	0.0009	846	0.00083	657	
	0.0014	1280	0.00125	1022	
	0.0016	1526	0.00178	1552	
	0.0028	3033	0.00240	2100	
NaOD	0.0005	485	NaOD	0.00329	3089
	0.0008	739	0.00045	242	
	0.0010	898	0.00096	696	
	0.0185	1636	0.00163	1555	
	0.0019	1783	0.00261	2733	

**Fig. 1** pH-Rate profiles for compounds **3a** (□), **3f** (■) and **3g** (●) at 25 °C.**Fig. 2** pH-Rate profiles for compounds **3a** (□), **3b** (△), **3c** (○), **3d** (●) and **3e** (■) at 25 °C.

base catalysis at higher pH values. Compound **3f**, in which the amino group is one atom further removed from the carbonyl group, also displays a sigmoid-shaped curve but the effect is much less pronounced. As will be shown later, this is because there is a smaller difference in reactivity between the protonated and unprotonated forms of **3f** than there is between the analogous forms of **3a**. Fig. 2 contains the pH-rate profiles for the different α -aminoacyl derivatives **3a–e**; all compounds exhibit sigmoid curves, but the reactivity varies with the structure of the amino acid side-chain.

Sigmoid-shaped pH-rate profiles have been observed for amino acid esters^{7–13} and aminoacyl RNA⁷ and have been interpreted by mechanisms involving attack by HO⁻ on both the conjugate acid of the amino acid ester as well as on the free ester. At pH values below the pK_a of the amino group reaction with the conjugate acid predominates; at pH values higher than the pK_a, the neutral species predominates.



Scheme 2

Above pH 3, the kinetically relevant processes for the triazenes **3** are shown in Scheme 2. Based on these, the following expression for k'_{obs} can be deduced:

$$k'_{\text{obs}} = (k_1[\text{H}^+]^2[\text{H}_2\text{O}] + k_2K_w[\text{H}^+] + k_3K_aK_w) / \{(K_a + [\text{H}^+])[\text{H}^+]\} \quad (1)$$

where K_a is the acid dissociation constant for the protonated aminoacyltriene, K_w is ionic product of water and k_1 , k_2 and k_3 are the second-order rate constants for the processes depicted in Scheme 2. The best computer fit (solid lines) to the experimental data (individual points) in Figs. 1 and 2 was achieved using eqn. (1), the experimentally determined values for k'_{obs} and pH, and the values for k_1 , k_2 , k_3 and $\text{p}K_a$ listed in Table 3. For **3a**, the ratio $k'_{\text{obs}}/[\text{HO}^-]$ was calculated across the pH range studied (Table 4). The ratio changes with pH reflecting the differing contributions of the kinetically relevant processes at each pH. At pH = 6.9, the $k'_{\text{obs}}/[\text{HO}^-]$ ratio equals the computer determined value for k_2 since, at that pH, the substrate is totally protonated and the reaction of HO^- with the protonated substrate is the most important process. Above pH 10, the ratio equals the computer determined value for k_3 , since the dominant process in this pH range is the attack of HO^- on the unprotonated substrate.

Table 3 Second-order rate constants for the hydrolysis of aminoacyltriazenes at 25 °C

	$k_{\text{obs}}/10^{-9} \text{ M}^{-1} \text{ s}^{-1}$	$k_2/\text{M}^{-1} \text{ s}^{-1}$	$k_3/\text{M}^{-1} \text{ s}^{-1}$	$\text{p}K_a$
3a	1.9	375	8.3	8.09 (7.78 ^b) (8.02 ^c)
3b	1.2	350	5.5	7.41 (7.05 ^b) (7.22 ^c)
3c	1.0	75	7.5	7.90 (7.66 ^b) (7.99 ^d)
3d	0.34	57	1.2	8.18 (7.49 ^b) (8.00 ^e)
3e	0.2	35	0.85	8.08 (7.54 ^b) (7.80 ^e)
3f	0.22	16	2.0	9.20 (9.13 ^f)
3g	0.94 ^a	—	4.2	—

^a For **3g** k_1 refers to the reaction of H_2O with the neutral substrate. ^b $\text{p}K_a$ of the corresponding amino acid methyl ester (ref. 9). ^c $\text{p}K_a$ of the corresponding amino acid amide (ref. 14). ^d $\text{p}K_a$ of the corresponding amino acid amide (ref. 15). ^e $\text{p}K_a$ for leucinamide (ref. 14). ^f $\text{p}K_a$ of the corresponding amino acid ethyl ester (ref. 16).

Table 4 Observed catalytic bimolecular rate constants for **3a**

pH	$k'_{\text{obs}}/10^{-5} \text{ s}^{-1}$	$k'_{\text{obs}}/[\text{HO}^-] \text{ M}^{-1} \text{ s}^{-1}$
5.26	0.061	335
6.93	3.20	376
7.35	8.50	379
8.63	35.9	84
10.36	172.3	7.5
10.56	299	8.2
10.84	700	10.1
11.25	1400	7.9
11.31	1690	8.3
11.43	2230	8.3

$\text{p}K_a$ values

The calculated $\text{p}K_a$ values for the α -amino acid derivatives (Table 3) are between 0.2 and 0.7 units above those reported for the corresponding methyl esters⁹ (for the β -amino acid derivative this difference in $\text{p}K_a$ values is very small), and roughly two $\text{p}K_a$ units lower than those of the parent amino acids. This effect has been attributed to a difference in ΔS° for the ionisation process.⁹ For the amino acids, ionisation involves a change from a neutral species to two ions ($^+\text{NH}_3\text{CHR}\text{COO}^- \rightarrow \text{NH}_2\text{CHR}\text{COO}^- + \text{H}_3\text{O}^+$) and will involve a more negative ΔS° than the ion-ion change in the esters ($^+\text{NH}_3\text{CHR}\text{COOMe} \rightarrow \text{NH}_2\text{CHR}\text{COOMe} + \text{H}_3\text{O}^+$).⁹ Our compounds have the same type of dissociation (ion-ion), so we would expect a similar effect. The slightly higher $\text{p}K_a$ values of the aminoacyltriazenes compared with amino acid esters are probably due to a smaller $-I$ inductive effect of the acyltriene moiety. Indeed, the $\text{p}K_a$ values of the aminoacyltriazenes more closely follow those of the corresponding amino acid amides.^{14,15}

Relative magnitudes of k_1 , k_2 and k_3

The bimolecular rate constants, k_1 , for the reaction of water with the protonated substrate are very small, reflecting the low nucleophilicity of water. Comparison of the k_1 value for **3c** with those for the analogous glycol derivatives of paracetamol ($1.01 \times 10^{-7} \text{ M}^{-1} \text{ s}^{-1}$ at 25 °C¹⁰) and benzyl alcohol ($3 \times 10^{-8} \text{ M}^{-1} \text{ s}^{-1}$ at 60 °C¹³) reveals that, for the k_1 process, aminoacyltriazenes are about as reactive as simple amino acid esters (allowing for temperature differences) but about 100-fold less reactive than the corresponding aryl esters.

The process involving attack of HO^- on the protonated substrate, k_2 , is $ca. 10^{11}$ more favoured than k_1 . Similar rate enhancements ($2-3 \times 10^9$) have been observed for glycol esters,^{10,13} but those determined for the aminoacyltriazenes, $ca. 7.5 \times 10^{10}-3 \times 10^{11}$, are somewhat larger. Again, a comparison of the k_2 value for the glycol compound **3c** with those for the glycol esters of ethanol ($28.3 \text{ M}^{-1} \text{ s}^{-1}$ at 25 °C⁹), paracetamol ($3120 \text{ M}^{-1} \text{ s}^{-1}$ at 25 °C¹⁰) and metronidazole (2-methyl-5-nitroimidazole-1-ethanol) ($158 \text{ M}^{-1} \text{ s}^{-1}$ at 25 °C¹¹) reveals the aminoacyltriazenes to be as reactive as alkyl esters of amino acids but $ca. 50$ times less reactive than aryl esters. As expected, the k_2 value for **3c** is larger than for **3f**, consistent with a greater electron-withdrawing effect of the NH_3^+ group in the former. Surprisingly, however, the k_2 value for the glycol derivative **3c** is only slightly larger than those for the α -substituted compounds **3d** and **3e**, and it is somewhat smaller than those of the other α -substituted compounds **3a** and **3b**. We comment on this below.

For the α -aminoacyl compounds, the rate constants for the reaction between the neutral substrate and HO^- , step k_3 , are between 10- and 60-fold smaller than the corresponding values for the protonated substrate. For the α -alanyl derivative **3a**, the ratio k_2 to k_3 is $ca. 38$; for the glycol derivative the corresponding ratio is 10. These differences are of the same order of magnitude as those found for glycine methyl ester (45),¹² glycine ethyl ester (22)⁹ and glycine benzyl ester (70),¹³ but somewhat smaller than those observed for the glycol ester of paracetamol (130)¹⁰ and the various amino acid esters of metronidazole (60–230).¹¹ Not surprisingly, for the β -alanyl derivative **3f**, in which the $\text{NH}_2/\text{NH}_3^+$ group is one atom further removed from the carbonyl carbon atom and its electronic effect correspondingly diminished, the k_2 to k_3 ratio (6) is somewhat smaller. These rate enhancements, which have also been observed for reactions between HO^- and esters containing a cationic centre,^{13,17} have been accounted for by postulating favourable electrostatic interactions in the transition state. The k_3 reactivity differences between the compounds (Table 3) roughly parallels those observed for the corresponding k_2 values. Interestingly, the k_3 values reveal the N -acetyl derivative

Table 5 Solvent kinetic deuterium isotope effects for the hydroxide ion and buffer-catalysed hydrolyses of compounds **3a** and **3c**

Compound	Buffer	pH (pD)	$k'_{\text{obs}}/10^{-6} \text{ s}^{-1}$	$k_2^{\text{H}}/k_2^{\text{D}}$	$k'_B/10^{-6} \text{ M}^{-1} \text{ s}^{-1}$	$k_B^{\text{H}}/k_B^{\text{D}}$
3a	Imidazole-H ₂ O	6.51	6.42		15.3	
	Imidazole-D ₂ O	(6.68)	1.62	0.8	6.0	1.38
3c	Imidazole-H ₂ O	6.52	1.87		5.94	
	Imidazole-D ₂ O	(6.68)	0.39	0.96	2.48	1.27

3g to have a reactivity similar to the unprotonated form of the α -aminoacyl compounds.

Solvent deuterium isotope effects

For **3a** and **3c**, k_{obs} values were also determined in D₂O using imidazole buffers (Table 1) and NaOD (Table 3). In the buffer solutions, the dominant, buffer-independent, reaction is k_2 , the attack of hydroxide on the protonated substrate, and eqn. (1) can be simplified to:

$$k'_{\text{obs}} = k_2 K_w / (K_a + [\text{H}^+]) \quad (2)$$

Consequently, the observed solvent deuterium isotope effect is given by:

$$k'_{\text{obs}}^{\text{H}}/k'_{\text{obs}}^{\text{D}} = k_2^{\text{H}} K_w^{\text{H}} (K_a^{\text{D}} + [\text{D}^+]) / k_2^{\text{D}} K_w^{\text{D}} (K_a^{\text{H}} + [\text{H}^+]) \quad (3)$$

By rearrangement of eqn. (3), the solvent deuterium isotope effect for the bimolecular reaction of HO⁻ with the protonated substrate, $k_2^{\text{H}}/k_2^{\text{D}}$, is given by:

$$k_2^{\text{H}}/k_2^{\text{D}} = k'_{\text{obs}}^{\text{H}} K_w^{\text{D}} (K_a^{\text{H}} + [\text{H}^+]) / k'_{\text{obs}}^{\text{D}} K_w^{\text{H}} (K_a^{\text{D}} + [\text{D}^+]) \quad (4)$$

The buffer-independent k'_{obs} values are contained in Table 5; the $\text{p}K_a$ values for **3a** and **3c** in H₂O are contained in Table 3, and the corresponding $\text{p}K_a$ values in D₂O were calculated to be 8.61 and 8.42, respectively, using isotopic fractionation factors.¹⁸ The solvent deuterium isotope effects, $k_2^{\text{H}}/k_2^{\text{D}}$, for **3a** and **3c** in pH 6.5 imidazole buffers are then calculated to be 0.8 and 0.96, respectively.

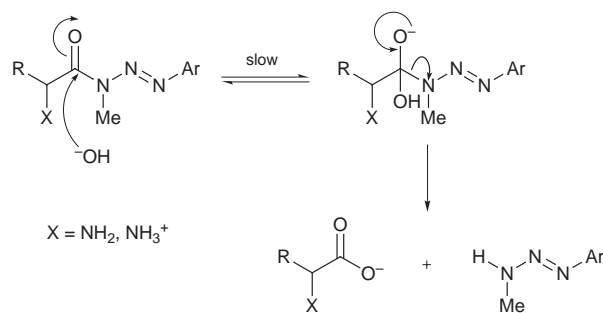
In NaOD solutions, the dominant reaction is k_3 and the observed pseudo-first-order rate constant is given by:

$$k_{\text{obs}} = k_3 [\text{DO}^-] \quad (5)$$

The data in Table 2 give rise to values of k_3^{H} and k_3^{D} of 8.3 and 9.23 M⁻¹ s⁻¹, respectively, for **3a** and of 8.57 and 9.38 M⁻¹ s⁻¹, respectively, for **3c**. The solvent deuterium isotope effects, $k_3^{\text{H}}/k_3^{\text{D}}$, for **3a** and **3c** are thus both 0.9.

Mechanism of the HO⁻-catalysed reactions

α -Aminoacyltriazenes exhibit a reactivity towards HO⁻ that is very similar to the corresponding amino acid methyl esters.⁹ This is consistent with data previously obtained for acyltriazenes which demonstrated that these compounds behave more like esters than amides.⁶ Therefore, the mechanism of hydrolysis involves rate-limiting formation of a tetrahedral intermediate *via* reaction of HO⁻ with either the protonated or unprotonated α -aminoacyltriene (Scheme 3). The solvent deuterium isotope effects on both k_2 and k_3 are entirely consistent with such nucleophilic attack of HO⁻ at the acyl carbon atom. The formation of the tetrahedral intermediate involves an increase in steric congestion, so smaller rate constants for the compounds with bulkier substituents might be expected. Indeed, the valyl and isoleucyl derivatives **3f** and **3g** are the least reactive of the compounds studied. However, by this reasoning the glycyl derivative **3c** appears to be much less reactive than expected, though similar behaviour has been observed before



Scheme 3

for the corresponding amino acid esters of metronidazole.¹¹ Indeed, the k_2 values for compounds **3a–e** correlate with the corresponding values for the equivalent derivatives of metronidazole according to eqn. (6).

$$k_2^{\text{triaz}} = 0.81 k_2^{\text{met}} - 9.4 \quad (r^2 = 0.97, n = 5) \quad (6)$$

Thus, although the reason(s) for the low reactivity of the glycyl derivatives remain unclear, similar factors must affect the hydrolysis of both series of compounds. Presumably solvent organisation around the aminoacyl moiety is important.

A similar, though poorer, correlation exists for the corresponding k_3 values [eqn. (7)], but whereas the triazene

$$k_3^{\text{triaz}} = 1.83 k_3^{\text{met}} + 1.2 \quad (r^2 = 0.64, n = 5) \quad (7)$$

derivatives are less reactive than the metronidazole esters in the k_2 process they are the more reactive in the k_3 process. We are currently unable to account for this reversal of reactivity.

The buffer-catalysed reaction

From the data in Table 1, it is apparent that the hydrolysis of the aminoacyltriazenes is buffer-catalysed across the pH range. At pH values >1 unit below the $\text{p}K_a$ of the triazene, the buffer catalyses the hydrolysis of the protonated substrate, which is the predominant form in such solutions. Conversely, at pH values >1 unit above the triazene $\text{p}K_a$ the substrate exists predominantly in the unprotonated form and it is this that suffers buffer-catalysed hydrolysis. In solutions where $\text{pH} \approx \text{p}K_a$ (e.g. for **3a**, morpholine buffers) both forms are present and both types of buffer catalysis are present. When predominantly one form of the substrate is present, pseudo-second-order rate constants for the buffer-catalysed reaction, k'_B , can be determined from the slopes of plots of k_{obs} versus $[\text{B}]_t$, where $[\text{B}]_t$ is the total concentration of the buffer used. For the same buffer system these slopes increase with increasing pH, and for different buffers with the $\text{p}K_a$ of the buffer, indicating that the catalytic species is the free-base form of the buffer. The true catalytic rate constants, k_B , are calculated from k'_B by dividing by the fraction of the basic form of the buffer present. Values for **3a** are shown in Table 6. When both forms of the substrate are present, it can be shown that:

$$k'_B = k_B^{\text{prot}} f_b^{\text{buffer}} f_a^{\text{triaz}} + k_B^{\text{unprot}} f_b^{\text{buffer}} f_b^{\text{triaz}} \quad (8)$$

Table 6 Second-order rate constants, k_B , for the buffer-catalysed hydrolysis of **3a** at 25 °C

Buffer	p <i>K</i> _a	$k_B/10^{-5} \text{ dm}^3 \text{ mol}^{-1} \text{ s}^{-1}$
Formate	3.61	0.26 ^a
Acetate	4.62	1.2 ^a
Pyridine	5.09	0.69 ^a
Imidazole	7.09	7.46 ^a
Phosphate	7.35	196 ^a
Morpholine	8.47	125 ^a 105 ^b
Me ₄ pip ^a	11.21	62500 ^b
Piperidine	11.26	69200 ^b

^a For the protonated substrate. ^b For the unprotonated substrate.

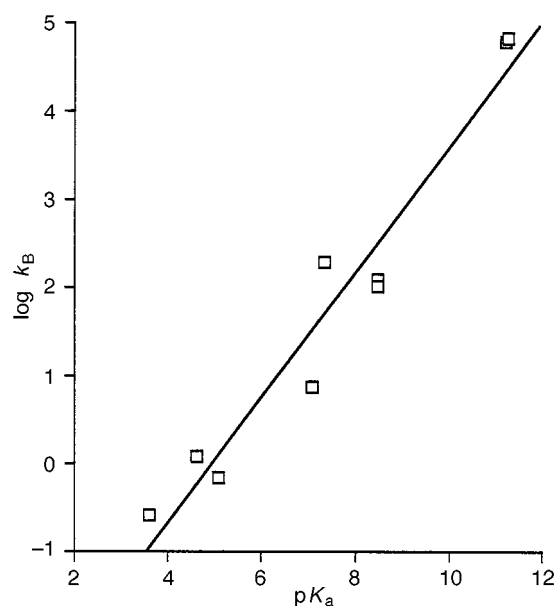
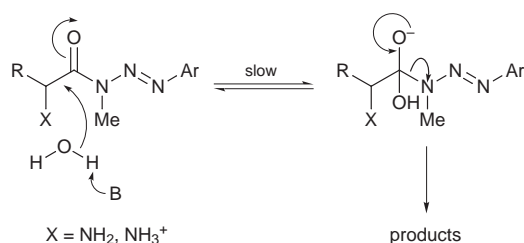


Fig. 3 Brønsted plot for the buffer-catalysed hydrolysis of **3a**.

where k_B^{prot} and k_B^{unprot} are the rate constants for the buffer-catalysed hydrolyses of the protonated and unprotonated forms of the substrate, and f_a and f_b are the fractions of the acidic and basic forms of the appropriate species present in the medium. Determination of k'_B at two different pH values enables k_B^{prot} and k_B^{unprot} to be calculated. Both values for the catalysis of **3a** by morpholine are also contained in Table 6.

A Brønsted plot of the data in Table 6 is shown in Fig. 3. Despite the scatter, the points define a line of slope *ca.* 0.65. One remarkable feature of this is that a single line appears to correlate data for both the protonated and unprotonated forms of the substrate. We are not clear why this should be so given the significant differences in the reactivity of these two species towards HO⁻ (*vide supra*), but it would imply that both reactions proceed through a similar mechanism. The Brønsted value of 0.65 is consistent with the buffer acting as a general-base catalyst (Scheme 4). For buffer catalysis of the hydrolysis



Scheme 4

of the unprotonated substrate, comparison of the data for piperidine and the sterically-hindered 2,2,4,4-tetramethylpiperidine reveals the two to have almost identical reactivity, implying that catalysis is of the general-base, rather than nucleophilic, type. Similarly for the protonated substrate, a comparison of the data for the imidazole-catalysed reaction in H₂O and D₂O (Table 5) using eqn. (9), where K_B^H and K_B^D

$$k_B^H/k_B^D = k'_B K_B^D [D^+] (K_a^H + [H^+]) (K_B^H + [H^+]) /$$

$$k'_B K_B^H [H^+] (K_a^D + [D^+]) (K_B^D + [D^+]) \quad (9)$$

are the K_a values for imidazole in H₂O and D₂O respectively (the latter calculated from K_B^H using fractionation factors¹⁸), gives rise to a solvent deuterium isotope effect, k_B^H/k_B^D , of *ca.* 1.4. A similar calculation for **3c** gives a value of *ca.* 1.3. Again, these are consistent with the buffer acting as a general-base rather than nucleophilic catalyst.

Experimental

Apparatus

Melting points were determined using a Kofler camera Bock-Monoscop M and are uncorrected. IR spectra were recorded using a Perkin-Elmer 1310 spectrometer. All UV spectra were recorded using a Perkin-Elmer Lambda 2 spectrophotometer. The ¹H-NMR spectra were recorded in d₆-DMSO solutions using a Jeol JNM-EX 400 spectrometer; chemical shifts are given in ppm and all *J* values are given in Hz. FAB mass spectra were recorded using a VG Mass Lab 25-250 spectrometer. Elemental analyses were obtained from Medac Ltd., Brunel Science Park, Englefield Green, Egham, Surrey, UK.

Chemicals

All chemicals were reagent grade, except those used for kinetic studies and HPLC which were of analytical or LiChrosolv (Merck) grade.

Synthesis

Aminoacyltriazenes **3** were synthesised by previously reported methods.¹ The following are new compounds: **3d**: mp 220–1 °C; $\nu_{\text{max}}/\text{cm}^{-1}$ 2226, 1699; δ_{H} 0.92 and 1.0 (6H, dd, *J* 8, 2 × Me), 2.26 (1H, m, *J* 8, CHMe₂), 3.42 (3H, s, *N*-Me), 4.95 (1H, br m, α -CH), 7.85 (2H, d, *J* 8.8, Ar), 8.04 (2H, d, *J* 8.8, Ar), 8.63 (3H, br s, NH₃⁺); *m/z* 260 (MH⁺), 130, 102. Found: C, 52.7; H, 6.2; N, 23.4%. C₁₃H₁₇N₅O requires: C, 52.8; H, 6.1; N 23.7%. **3e**: mp 243–4 °C; $\nu_{\text{max}}/\text{cm}^{-1}$ 2226, 1695; δ_{H} 0.81 and 0.85 (3H, 2 × t, *J* 8, CH₂CH₃), 0.90 and 0.97 (3H, 2 × d, *J* 6.8, α -Me), 1.16 and 1.25 (1H, 2 × m, MeCHCH), 1.43 and 1.53 (1H, 2 × m, MeCHCH), 2.0 (1H, br m, MeEtCH), 3.40 (3H, s, *N*-Me), 5.02 (1H, m, α -CH), 7.82 and 7.86 (2H, 2 × d, *J* 8.9, Ar), 8.03 (2H, d, *J* 8.9, Ar), 8.40 (3H, br s, NH₃⁺); *m/z* 274 (MH⁺), 130, 102. Found: C, 54.1; H, 6.5; N, 22.45%. C₁₄H₁₈N₅O requires: C, 54.3; H, 6.5; N, 22.6%.

Kinetics

The decomposition of the aminoacyltriazenes was followed by monitoring the decrease in UV absorbance of the substrate at an appropriate wavelength. In general, reactions were monitored continuously in cells thermostatted to ± 0.1 °C. Pseudo-first-order rate constants were obtained from plots of $\ln(A_t - A_\infty)$ versus time, where A_t and A_∞ are the absorbance at time *t* and infinity, respectively. For very slow reactions, a discontinuous method, in which aliquots were taken from a stock reaction at timed intervals, was used. For these, reactions were followed to about 3 half-lives and an initial rate method was used to calculate the rate constants. The ionic strength of the reactions was maintained at 0.2 mol dm⁻³ by the addition of

NaClO₄. At the conclusion of each experiment the pH of the reaction solution was measured. pD values were calculated using the expression $pD = pH + 0.4$.¹⁹

Product analysis

The UV spectra of the reaction solutions at the conclusion of each experiment were identical with those of the corresponding anilines. In selected cases the anilines were isolated from large scale reactions.

Acknowledgements

This work was supported by JNICT and PRAXIS XXI, project n°2/2.1/SAU/1404/95.

References

- 1 Part 15: E. Carvalho, J. Iley, M. de J. Perry and E. Rosa, *Pharm. Res.*, 1998, **15**, 931.
- 2 V. S. Lucas and A. T. Huang, in *Chemical Management of Melanoma*, ed. H. F. Seigler, Martinus Nijhoff, The Hague, 1982.
- 3 T. A. Connors, P. M. Goddard, K. Merai, W. C. J. Ross and D. E. V. Wilman, *Biochem. Pharmacol.*, 1976, **25**, 241.
- 4 M. Julliard and G. Vernin, *Ind. Eng. Chem. Prod. Res. Rev.*, 1981, **20**, 287.
- 5 J. Iley, G. Rucroft, E. Carvalho and E. Rosa, *J. Chem. Res. (S)*, 1989, 162.
- 6 E. Carvalho, J. Iley and E. Rosa, *J. Chem. Soc., Perkin Trans. 2*, 1993, 865.
- 7 R. Wolfenden, *Biochemistry*, 1963, **2**, 1090.
- 8 R. W. Hay, L. J. Porter and P. J. Morris, *Aust. J. Chem.*, 1966, **19**, 1197.
- 9 R. W. Hay and L. J. Porter, *J. Chem. Soc. (B)*, 1967, 1262.
- 10 I. M. Kovach, I. H. Pitman and T. Higuchi, *J. Pharm. Sci.*, 1981, **70**, 881.
- 11 M. J. Cho and L. C. Haynes, *J. Pharm. Sci.*, 1985, **74**, 883.
- 12 M. R. Wright, *J. Chem. Soc. (B)*, 1968, 548.
- 13 E. Jensen and H. Bundgaard, *Int. J. Pharm.*, 1991, **71**, 117.
- 14 W. P. Jencks and J. Regenstein, 'Ionization Constants of Acids and Bases', in *Handbook of Chemistry and Molecular Biology*, 3rd edn., vol. 1, ed. G. D. Fasman, CRC Press, Cleveland, OH, 1976, p. 305.
- 15 S. P. Datta and B. R. Rabin, *Trans. Faraday Soc.*, 1956, **52**, 1117.
- 16 J. T. Edsall and M. H. Blanchard, *J. Am. Chem. Soc.*, 1933, **55**, 2337.
- 17 B. Holmquist and T. Bruice, *J. Am. Chem. Soc.*, 1969, **91**, 2985.
- 18 N. S. Isaacs, *Physical Organic Chemistry*, Longman, Harlow, 1987.
- 19 R. G. Bates, *Determination of pH*, Wiley, New York, 1954.

Paper 8/05704D